INFN Istituto Nazionale di Fisica Nucleare

ISTITUTO NAZIONALE DI FISICA NUCLEARE

Laboratori Nazionali di Frascati

INFN-13-10/LNF
2nd July 2013

Manifold Design of the GEM Detectors for a Uniform Gas Flow

G. Raffone

INFN-Laboratori Nazionali di Frascati Via E. Fermi 40, I-00044 Frascati, Italy

Abstract

A simple design solution of manifolds is suggested to get nearly uniform flow of the gas mixture inside the GEM chamber. Analytical expressions concerning the design of the piping system are derived and numerically checked by means of the ANSYS-FLOTRAN code v.13 [1]. A full gas flow CFD simulation of the trapezoidal detector is finally performed on the basis of the proposed formulae that should be thoroughly validated only by further experimental tests.

*Published by **SIDS–Pubblicazioni***
Laboratori Nazionali di Frascati

1 – Introduction.

Uniform and vortex free flow inside GEM chambers is highly recommended to avoid regions where contaminants are accumulated or trapped in; in [2] the effect of some grooves in the aluminium frame are simulated as well as the benefits of multiple inlets and outlets; the present solution is, in some way, an improvement of that design keeping in mind the following criticisms:

a) the cross section of the grooves (about 1 mm²) is of the same order of that of the holes through which the gas mixture is injected into the chamber; then the pressure losses between two adjacent holes is considerably high and the gas flow path will privilege those holes closer to inlets (or outlets) anyway; then the resulting flow inside the chamber is far to be uniform;
b) multiple inlets and outlets (flow parallelization) may weaken the effects of a) but they never overcome them; the doubling of all the hydraulic circuits is a little bit difficult not only for the available room but, above all, because the pressure of all of them must be well balanced for each chamber (otherwise there will be always one favourite inlet or outlet); a flow serialization does not have any of these drawbacks;
c) recirculation regions between any two adjacent holes (in the chamber side) may develop even at very low Reynolds numbers.

Nevertheless the small room of the grooves is important for the budget of the available surface of the detector; it will be shown that a well dimensioned manifold will take from 10 to 20 mm along the two sides of the chamber and the geometric design should be revisited in some way.

2 – A pipe with a lateral slot as a nearly uniform flow source.

The proposed design is very simple (see Fig. 1): a single inlet (or outlet) is made of a manifold (a straight pipe of length L, large equivalent diameter $D_{eq.}$ and low pressure loss $\Delta p_{manifold}$) and a nozzle (a lateral slot of small height H, width W and high pressure loss Δp_{nozzle}); that nozzle replaces the row of holes; the manufacturing of the manifold is not expensive also (may be an extruded aluminium tube having a Ω shape cross section with high precision spacers of height H); the manifold pressure loss $\Delta p_{manifold} = p_1 - p_2$ is computed between $z = 0$ (p_1: manifold inlet pressure) and $z = L$ (p_2: manifold closed end pressure, fluid at rest) while the nozzle pressure loss $\Delta p_{nozzle} = p_2 - p_n$ is computed at the closed end of the collector $z = L$ between $x = 0$ (nozzle entrance) and $x = W$ (nozzle escape); the pressure p_n downstream the nozzle is assumed to be constant (i.e. independent on z).

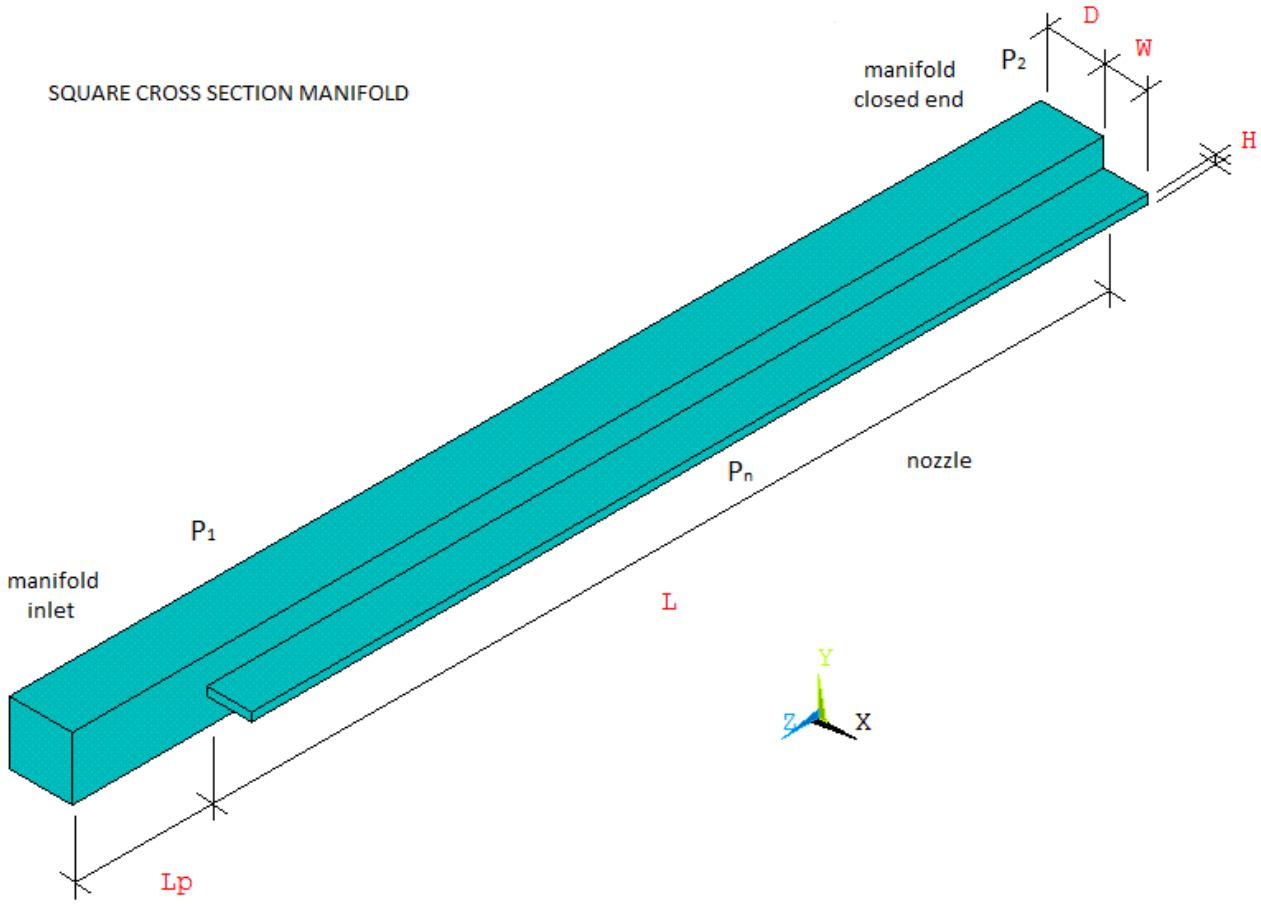

Figure 1 – Manifold layout.

In terms of impedances the preferred gas flow path will be always that of the manifold (z direction) rather than that of the nozzle (x direction) if:

$$\Delta p_{manifold} \ll \Delta p_{nozzle} \qquad (1)$$

3 – Assumptions.

a) the flow is assumed to be laminar everywhere since the Reynolds numbers range is about 0.01 to 10 depending on the section and the flow rates; for such low Reynolds numbers the flow is said to be a creeping flow [3] (a Stokes flow) and the inertial forces can be neglected;

b) the kinetic energy is very small too and the difference between the total and the static pressure is negligible;

c) the recirculation regions are smaller and smaller as $Rey \to 0$ and the flow uniformity inside the chamber is the major design parameter rather than the vortex free field; nevertheless the design should take into account higher flow rates for which recirculation regions may develop in the proximity of sharp corners;

d) the flow is assumed to be incompressible and the body forces can be cancelled because there is no free surface and the density gradients are negligible as well as the thermal ones (the energy equation is ignored); then the density ρ and the dynamic viscosity μ are assumed to be independent on the temperature;

e) in a steady state flow the continuity equation consists in the null divergence of the velocity vector $\vec{\nabla} \cdot \vec{v} = 0$ and the momentum equation (the Navier-Stokes equation $\vec{\nabla} p = \mu \nabla^2 \vec{v}$) is reduced to $\nabla^2 p = 0$; then in a steady incompressible creeping flow the static pressure is harmonic; in two dimensions it is possible to introduce a bi-harmonic stream function that leads to a bi-potential flow problem; a similar

stream function can be derived also if the inertia terms are included and it is widely used also in the problems regarding with the boundary layer suction or injection (briefly referenced later in [3], [4] and [6]) as it happens in the proposed design.

4 – Transport properties of Ar-CO_2-CF_4 (45%-15%-40%) mixture.

The Ar-CO_2-CF_4 (45%-15%-40%) non polar gas mixture is assumed to be an ideal gas (molecular weight 59.8 kg/kmol) in the range of temperatures of interest; the following table shows the nominal conditions (273.15 K, 101325 Pa).

density ϱ	2.6670	kg/m³
kinematic viscosity ν	6.6797e-06	m²/s
dynamic viscosity μ	17.815e-06	kg/ms
thermal conductivity λ	14.991e-03	W/mK
thermal diffusivity α	8.830e-06	m²/s
Prandtl number Pr	0.756	-
gas constant R	139.04	J/kgK
constant pressure specific heat	636.12	J/kg/K
ratio of specific heats γ	1.280	-

In these thermodynamic conditions the mean free path of that mixture is 41.9 nm and the Knudsen number for a GEM foil hole (70 microns diameter) is Kn=0.0006; it follows that the gas flow through the GEM foil holes (if any) can be still considered continuous.

5 – Some useful Hagen-Poiseuille expressions.

The Hagen-Poiseuille expressions for circular and square sections (manifold, z axis) are given in (2), (3), for parallel plates (nozzle and chamber, x axis) in (4);

$$w_m = \left(\frac{D^2}{32\mu}\right)\frac{dp}{dz} \qquad \text{Rey} = \frac{\rho w_m D}{\mu} \qquad f_{Darcy} = \frac{64}{Rey} \qquad (circular) \quad (2)$$

$$w_m = \left(\frac{D^2}{28.45\mu}\right)\frac{dp}{dz} \qquad \text{Rey} = \frac{\rho w_m D}{\mu} \qquad f_{Darcy} = \frac{56.91}{Rey} \qquad (square) \qquad (3)$$

$$u_m = \left(\frac{H^2}{12\mu}\right)\frac{dp}{dx} \qquad \text{Rey} = \frac{2\rho u_m H}{\mu} \qquad f_{Darcy} = \frac{96}{Rey} \qquad (parallel) \quad (4)$$

In these expressions the subscript m refers to the mean velocity and f_{Darcy} is the Darcy friction factor (four times the Fanning); D is the diameter of the circular section or the side of the square section (the "equivalent diameter" $D_{eq.}$) while H is the distance between either the walls in the nozzle or the GEM foils in the chamber; the constant in (3) is given in (5) while the others are well known.

$$\frac{1}{28.45\ldots} = \frac{8}{\pi^4}\sum_{n=1,3,5,\ldots}^{+\infty}\frac{1}{n^4}\left[1 - \frac{2}{n\pi}tanh\left(\frac{n\pi}{2}\right)\right] \qquad (5)$$

6 – An extremely simplified analytic approach.

The boundary layer suction or injection is one of great relevance subject in fluid dynamics both from theory and application points of view; focusing the attention to the laminar boundary layer only, the pioneering work of Berman [4] was the starting point of analytical improvements during all these years and many of them are based on the above mentioned stream function to solve the momentum equation; in 2001 Karode [5] presented a brief but remarkable work showing that the gross balance of the volumetric flow rate in a porous channel agrees very well with the Berman solution; in other words a high level of approximation of the laminar boundary layer can be obtained without the direct integration of the Navier-Stokes equation by means of the stream function; the work of Karode is of great help and allows to build-up very simple and manageable expressions in the present design.

It must be underlined that there are some fundamental differences between the flow in the GEM manifold and that in the channel of Karode:

a) the boundary layer suction/injection is concentrated in the region close to the nozzle entrance in the former while it is equally distributed over the wetted perimeter in the latter; then the boundary layer in the GEM manifold loses the axial symmetry and it is substantially different from the one of Karode;
b) there are additional entrance pressure losses in the nozzle to be taken into account.

As far as a), at first glance, there is no reason to think that the gross balance of the volumetric flow rate does not work; there are local differences of the boundary layer in the cross section between the two flow fields and the problem is to investigate how the gross balance depends on them; for instance in [6] the suction/injection along only one wall of a square pipe in a laminar flow regime is solved on the basis of the Berman stream functions in conjunction with an integral continuity equation (see eq. 25 in [6]; it is a gross balance of the volumetric flow rate: the variation of the volumetric flow rate along the pipe equates the escaping volumetric flow rate through the single porous wall - the same assumption of Karode on the whole wetted perimeter); the reference [6] shows the complexity of such a flow: the present problem is even more complicated because the suction/injection is located only on a small part of the single wall of a square duct and any analytical solution requires a numerical integration anyway.

As far as b) the flow is an ultra-low Reynolds number flow and the entrance losses should be negligible as well as the entrance lengths (order of few hundreds of microns) before the boundary layer is fully developed in the nozzle [7]; then the following approach is expected to be fairly good only for very low Reynolds number and larger deviations are expected at higher and higher Reynolds number even in a pure laminar regime.

For both of the above reasons a CFD check is needed to verify that simplified analytical approach.

7 – Basic inequality.

From (2) and (3) the volumetric flow rate $Q(z)$ in the manifold is given in (6) where the constant B depends on the cross section.

$$Q(z) = -\left(\frac{D^4}{B\mu}\right)\frac{dp}{dz} \qquad \begin{cases} B = 128/\pi & (circular) \\ B = 28.45 & (square) \end{cases} \qquad (6)$$

Then, as Karode, the derivative (7) of the volumetric flow rate in the manifold equates the flow rate (per unit length) escaping the nozzle; the pressure losses are only expressed in terms of the Hagen-Poiseuille frictions as previously stated (i.e. no other kind of losses, such as the entrance losses, are taken into account).

$$\frac{dQ(z)}{dz} = -\left(\frac{D^4}{B\mu}\right)\frac{d^2p(z)}{dz^2} = -u_m(z)H \quad where \quad u_m(z) = \left(\frac{H^2}{12\mu}\right)\frac{p(z)-p_n}{W} \qquad (7)$$

Assuming that the nozzle downstream pressure p_n is constant (i.e. it does not depend on z) then the solution (9) of the second order linear differential equation (8) is easily obtained.

$$\frac{d^2p(z)}{dz^2} = \beta^2[p(z) - p_n] \quad where \quad \beta^2 = \frac{BH^3}{12WD^4} \tag{8}$$

$$p(z) = (p_1 - p_n)[cosh(\beta z) - tanh(\beta L)sinh(\beta z)] + p_n \tag{9}$$

The solution (9) satisfies the boundary conditions (10) where p_1 is the manifold inlet pressure and Q_1 is the total volumetric flow rate entering or leaving the manifold (11).

$$p(z)|_{z=0} = p_1 \quad \left.\frac{dp(z)}{dz}\right|_{z=0} = -\frac{B\mu}{D^4}Q_1 \quad \left.\frac{dp(z)}{dz}\right|_{z=L} = 0 \tag{10}$$

$$Q_1 = H\int_0^L u_m(z)dz = (p_1 - p_n)\frac{H^3}{12\mu W}\frac{tanh(\beta L)}{\beta} \tag{11}$$

And finally the manifold closed end pressure p_2 is given in (12).

$$p_2 = p(z)|_{z=L} = \frac{(p_1 - p_n)}{cosh(\beta L)} + p_n \tag{12}$$

It must be underlined that the nozzle mean escaping speed $u_m(z)$ has the same behavior of the manifold pressure $p(z)$, i.e. it is not constant even if the nozzle downstream pressure p_n is (CFD simulations show the correctness of that assumption if the flow has the same direction in both manifolds, i.e. inlet on left top and outlet on right bottom in a top view); by doing so the pressure profile of the outlet manifold $p(z)|_{out}$ is specular to the pressure profile of the inlet manifold $p(z)|_{in}$ and the pressure drop through the chamber is nearly constant for each streamline being $p_n|_{out}$ and $p_n|_{in}$ independent on z; the particles of the top streamline will accelerate from left to right while those of bottom one will decelerate; in other words the aim of both the manifolds is to lower as possible the component $\omega_y = \partial w/\partial x - \partial u/\partial z$ of the vorticity $\vec{\omega} = \vec{\nabla}\times\vec{v}$ in the inlet and outlet section of the chamber (see Fig. 2); by doing so each of the streamlines is in some way "forced" to be straight (an ideal manifold should have at the nozzle exit $w_m(z) = 0$, $u_m(z) = constant$ and $p_n = constant$ so $\omega_y \cong 0$ but only a rather expensive aerodynamic shaping of the cross section of the manifolds can fulfill all these requirements).

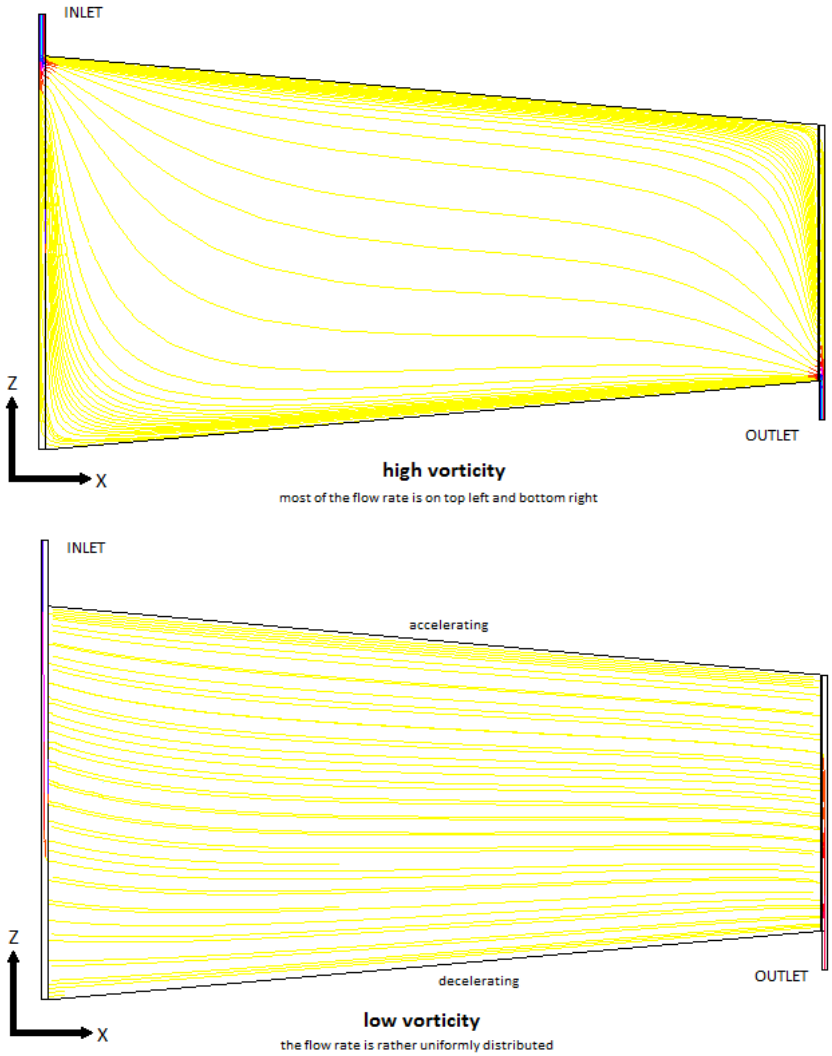

Figure 2 – The nozzle exit vorticity as the main design parameter for uniform gas flow.

Then the inequality (1) becomes $\beta L \ll ln(2+\sqrt{3})$ that is:

$$H^3 \ll H_{max}^3 = \frac{12\left[ln\left(2+\sqrt{3}\right)\right]^2}{B}\frac{WD^4}{L^2} \qquad (13)$$

For instance for a manifold of length $L = 500\ mm$, square side $D = 10\ mm$ and nozzle length $W = 5\ mm$ then a height of the nozzle H lower than $H_{max} \cong 0.53\ mm$ should give straight streamlines in the chamber.

The aim of following CFD simulations is to check the inequality (13) other than some of the previous equations as well as the nozzle entrance losses; it must be underlined that the inequality (13) involves only geometrical quantities, i.e. it does not depend on the flow as long as it is creeping, as above mentioned (it is valid only for very low Reynolds numbers); furthermore in (13) the diameter D plays the dominant role (fourth power).

8 – CFD tests on a single manifold.

A small manifold ($L = 100\ mm$, $D = 7\ mm$, $W = 5\ mm$, $H_{max} \cong 0.96\ mm$) has been tested in four configurations corresponding to two manifold Reynolds numbers (respectively 6 - creeping flow - and 100 - laminar but no more creeping) and to two H/H_{max} ratios (respectively 1 and 2); the volumetric flow rate was numerically computed at the manifold inlet and at the nozzle exit; the two values agree very well with (11) for $H/H_{max} = 1$

while there is a deviation for $H/H_{max} = 2$ more evident at high Reynolds; all the streamlines deviate from straight directions at the nozzle exit as the ratio H/H_{max} and/or the Reynolds number increase (see Fig. 3).

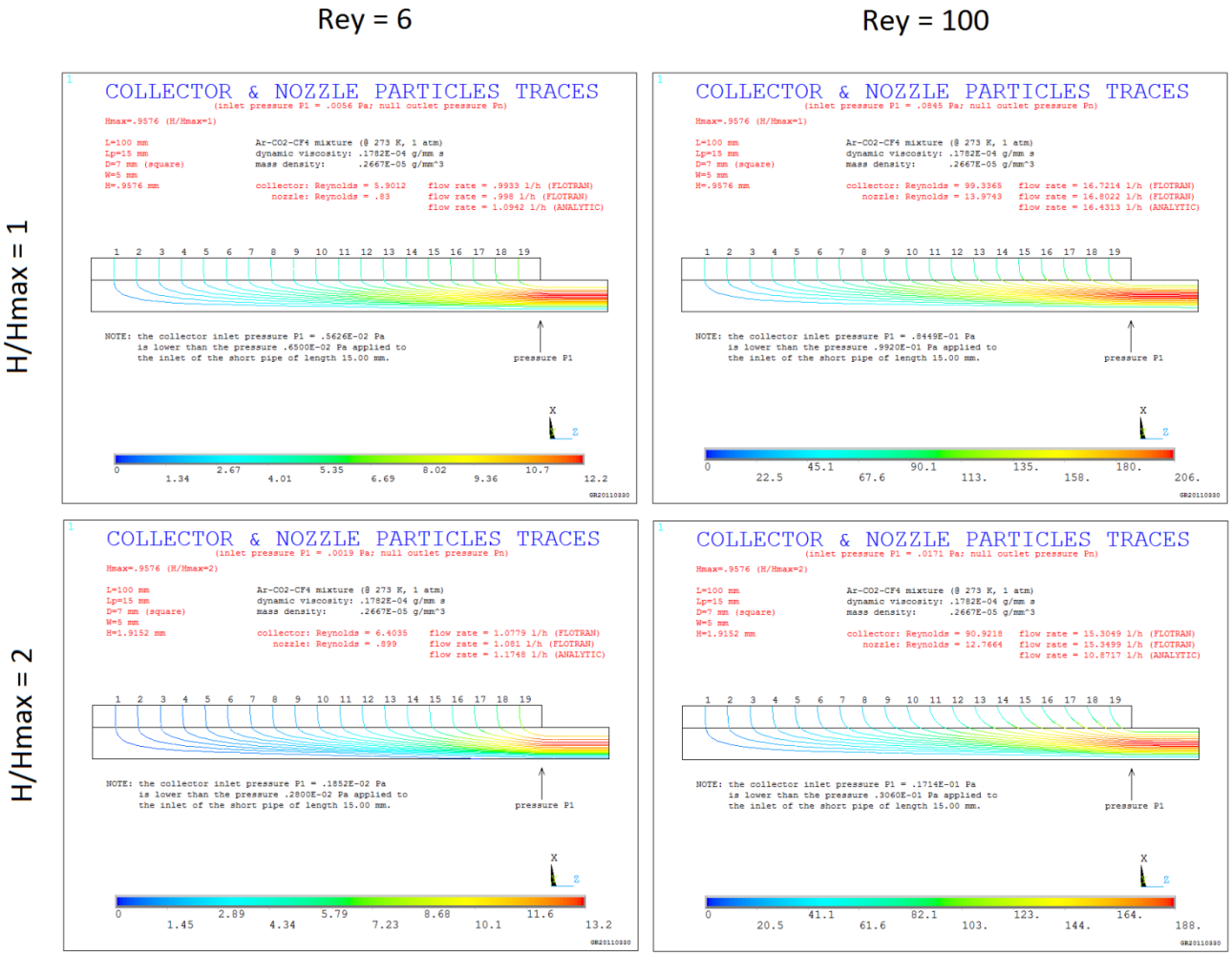

Figure 3 – Manifold particle traces.

Also the numerical pressure profile $p(z)$ of the manifold agrees very well with (9) for low Reynolds while some deviations are present at higher Reynolds (see Fig. 4); the entrance pressure losses seems to be small too only for low Reynolds; the bumps at the manifold inlet at high Reynolds are due to a vortex because of the inlet sharp edge (rounded profile recommended there).

Rey = 6 Rey = 100

H/Hmax = 1

H/Hmax = 2

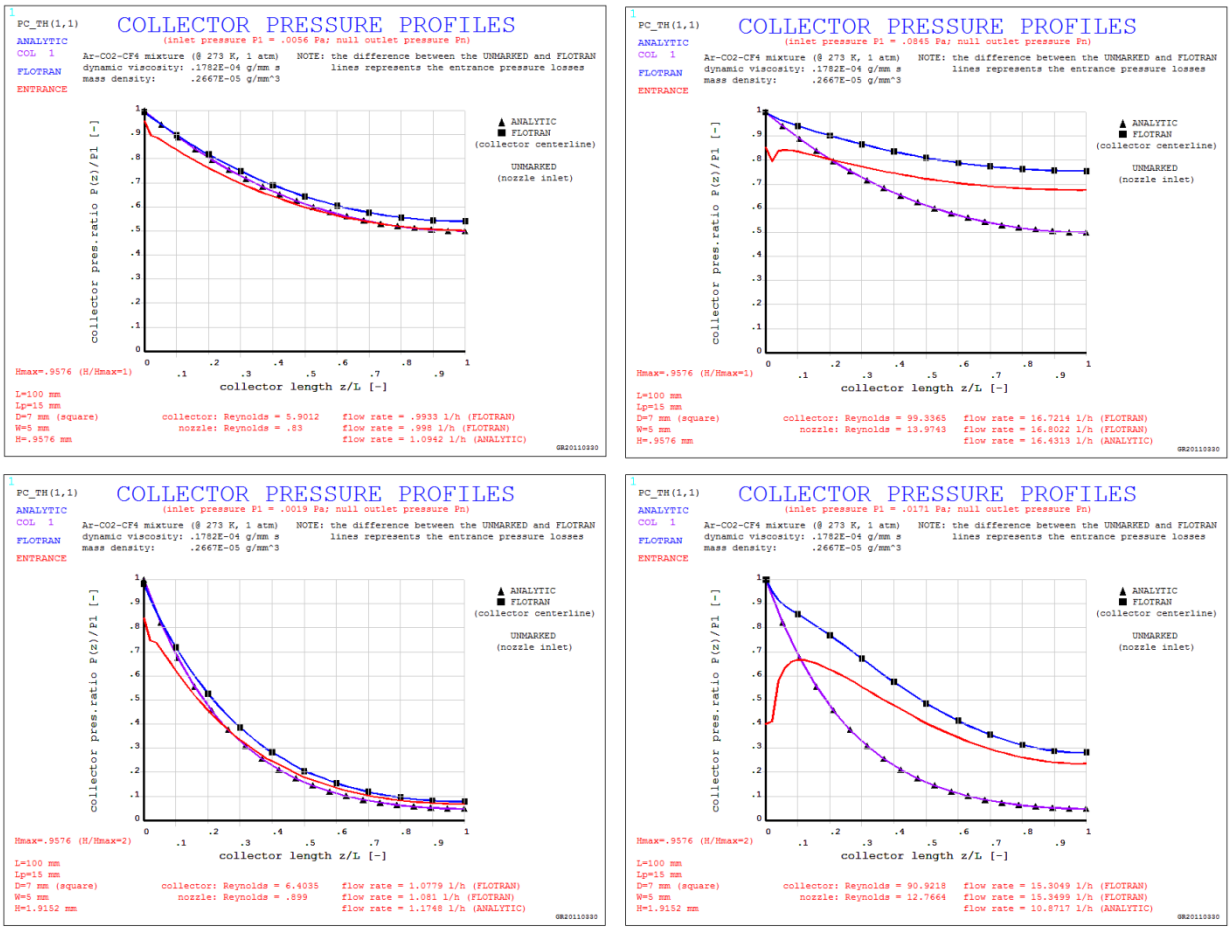

Figure 4 – Pressure profiles.

Furthermore the nozzle exit speed profiles agree very well with $u_m(z)$ in (7) for low Reynolds numbers (see Fig. 5); it must be pointed out that the derivatives $\partial u_m(z)/\partial z$ for $H/H_{max} = 1$ are much smaller than those for $H/H_{max} = 2$ meaning that *when the inequalities (1) and (13) are approached then a strong reduction of the vorticity is really achieved*; for higher Reynolds there are the usual deviations.

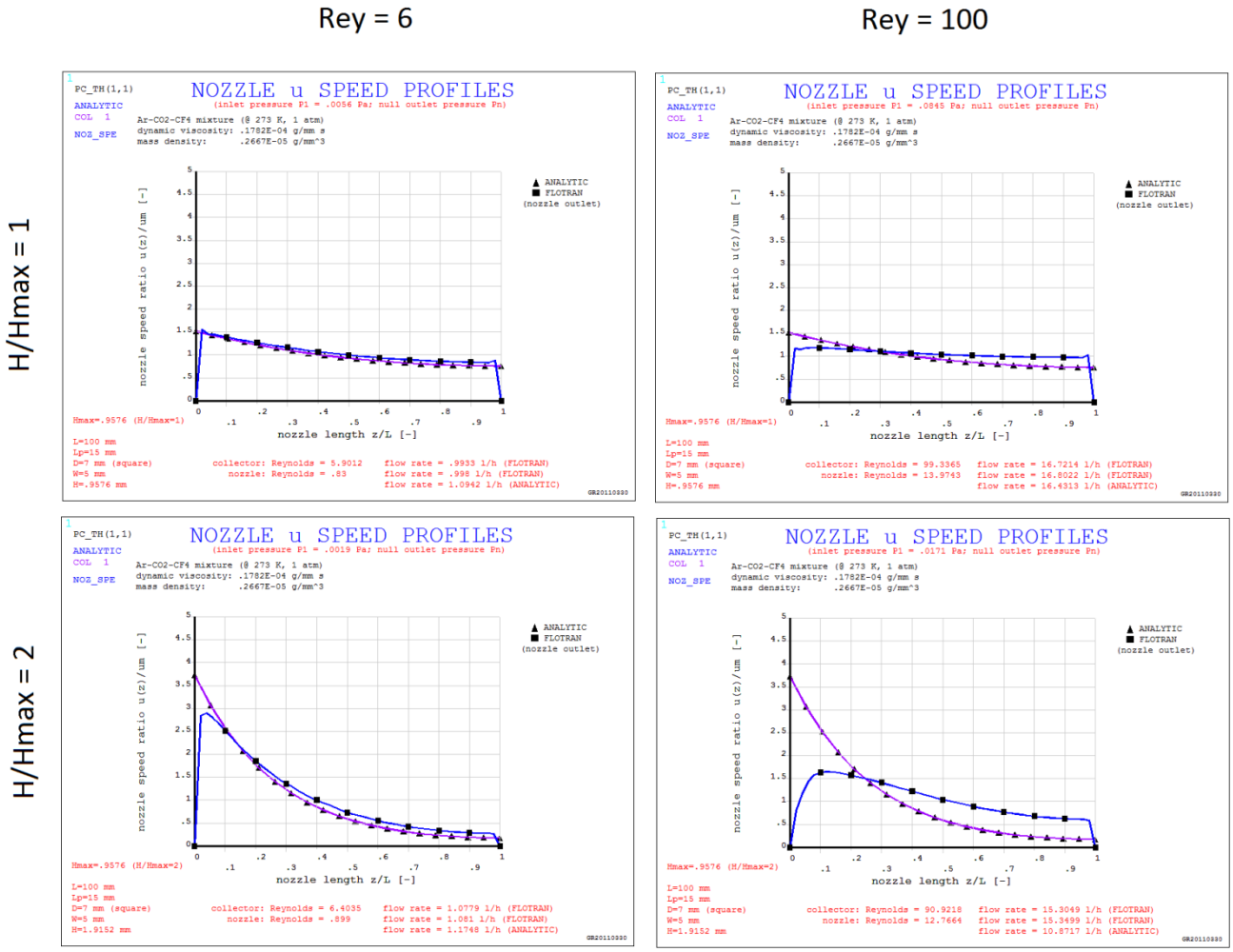

Figure 5 – Speed profiles.

9 – CFD test on a large square chamber.

A large rectangular chamber ($L = 530\,mm$, $D = 7\,mm$, $W = 5\,mm$, $H_{max} \cong 0.32\,mm$) of 1040 mm length was tested in the condition $H/H_{max} = 1$ (see Fig. 6); the volumetric flow rate is 0.25 l/h (about ¼ of that reported in [2] assuming three GEM foils equally 2 mm spaced); the streamlines are almost straight.

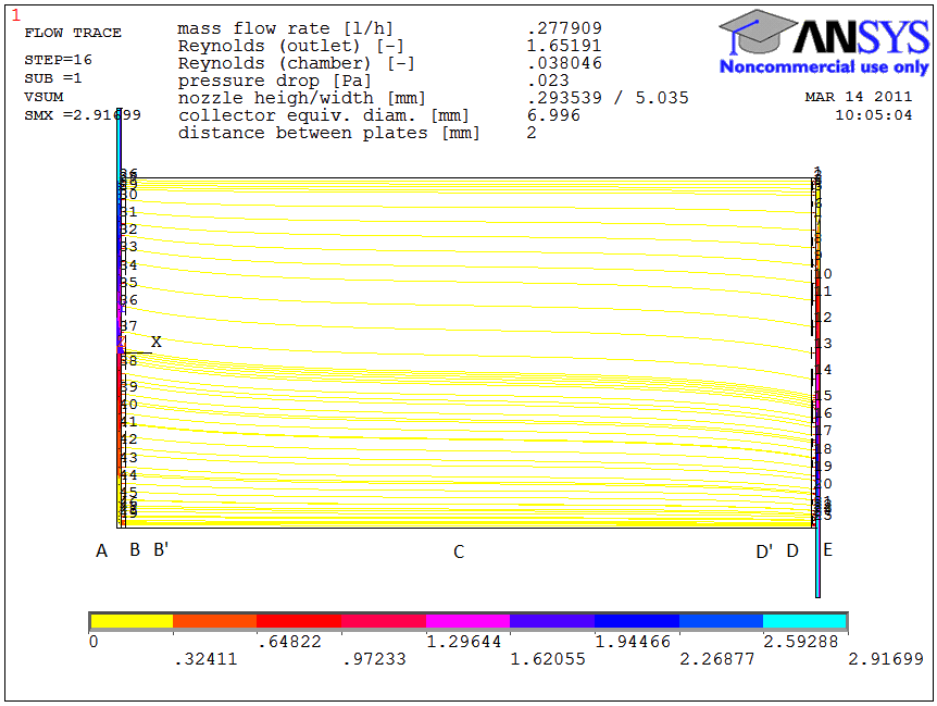

Figure 6 – CFD test on a rectangular chamber.

In Fig. 6 the sections A and E correspond to the manifolds centerlines, B and D to the nozzles ends (respectively the exit of the inlet nozzle and the entrance of the outlet nozzle), B' is a section just downstream the B section where the 2mm high chamber begins and D' is just upstream the D section where the 2mm high chamber ends; C is the section of the mid of the chamber.

The analysis shows that the pressure profiles in the sections B, C and D are constant, are previously assumed for the pressure p_n; in the section A and E they follows the pressure profile $p(z)$ of (9) (see Fig. 7).

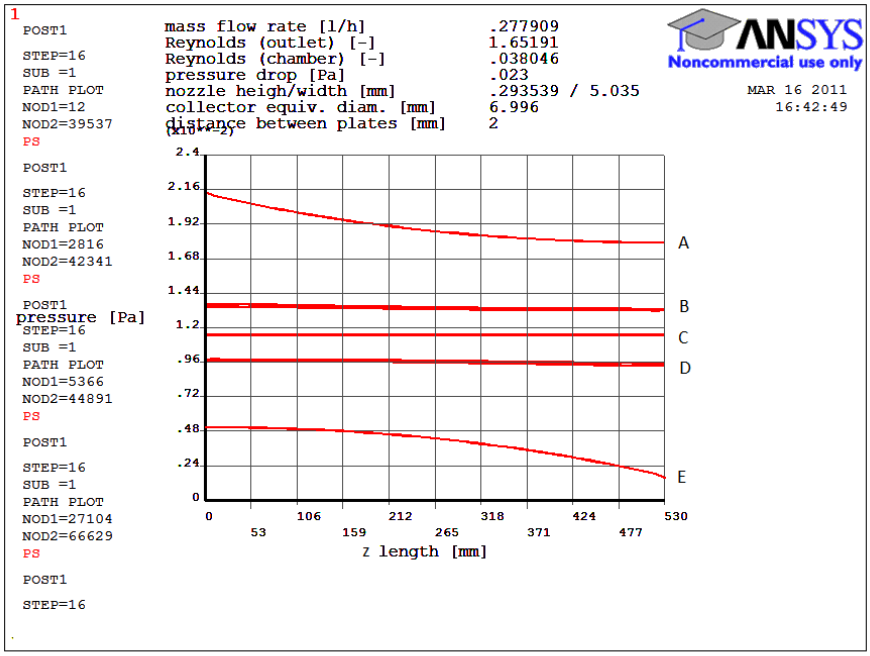

Figure 7 – Pressure profiles in the test chamber.

The $u_m(z)$ speed profiles follow the pressure profiles in the sections B and D; in the chamber that speed is almost constant and approach the value of 0.1 mm/s given in [2] – sections B', C and D' (see Fig. 8).

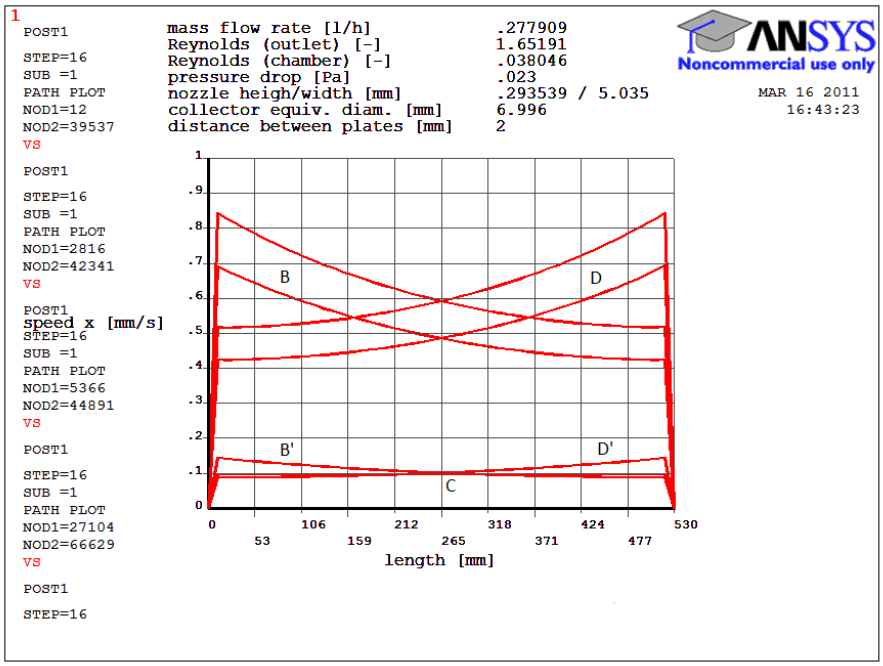

Figure 8 – Speed profiles in the test chamber.

10 – Conclusions.

That design seems to be fully confirmed by the previous analytical and computational analysis; experimental test on simple chambers should be carried out to check it; further CFD analysis should be extensively performed to improve geometry and other details.

References

[1] ANSYS® Release 13， Copyright© 2011 by SAS IP.

[2] S. Colafranceschi (2010), *Gas Flow Simulations for Gaseous Detectors*, Gaseous Detectors Poster N48-234, IEEE Conference (30 Oct. - 6 Nov. 2010), Knoxville, Tennessee (USA).

[3] Schlichting H. (1951), *Boundary Layer Theory*, Seventh Edition, McGraw-Hill Classic Textbook Reissue Series.

[4] A.S. Berman (1953), *Laminar flow in channels with porous walls*, J. Appl. Phys. 24 (9) (1953) 1232-1235.

[5] S.K. Karode (2001), *Laminar flow in channels with porous walls, revisited*, Journal of Membrane Science (Rapid communication) 191 (2001) 237-241.

[6] Y.Song and K.Sundmacher (2010), *Approximation of Laminar Flow Field in Rectangular Channels with Suction/Injection along One Wall*, Chem. Eng. Comm., 197 (2010) 551-570.

[7] R.Y.Chen (1973), *Flow in the entrance region at low Reynolds numbers*, J. Fluid Eng. (Trans. ASME) 95 (1973) 153-158.